

Synchrotron X-ray phase contrast imaging of leaf venation in soybean (*Glycine max*) after exclusion of solar UV (280–400 nm) radiation

A. Fatima,^{a*} S. Kataria,^b K. N. Guruprasad,^b A. K. Agrawal,^c B. Singh,^c P. S. Sarkar,^c T. Shripathi,^a Y. Kashyap^c and A. Sinha^c

Received 15 October 2015
Accepted 29 February 2016

^aUGC-DAE, Consortium for Scientific Research, University Campus, Khandwa Road, Indore (MP), India, ^bSchool of Life Sciences, DAVV, Khandwa Road, Indore (MP), India, and ^cNeutron and X-ray Physics Division, Bhabha Atomic Research Center, Trombay, Mumbai, India. *Correspondence e-mail: anees349@gmail.com

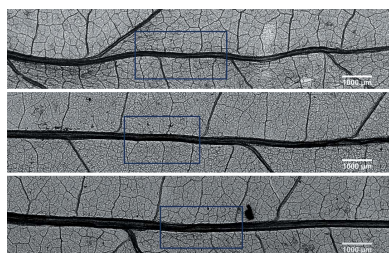
Edited by A. Momose, Tohoku University, Japan

Keywords: phase contrast imaging (PCI); micro-imaging; soybean; UV exclusion.

The hydraulic efficiency of a leaf depends on its vascular structure as this is responsible for transport activities. To investigate the effect of exclusion of UVAB and UVB radiation from the solar spectrum on the micro-structure of leaves of soybean (*Glycine max*, variety JS-335), a field experiment was conducted using synchrotron-based phase contrast imaging (PCI). Plants were grown in specially designed UV exclusion chambers, and wrapped with filters that excluded UVB (280–315 nm) or UVAB (280–400 nm), or transmitted all the ambient solar UV (280–400 nm) radiation (filter control). Qualitative observation of high-resolution X-ray PCI images obtained at 10 keV has shown the differences in major and minor vein structures of the leaves. The mid-rib width of the middle leaflet of third trifoliate leaves, for all treatments, were obtained using quantitative image analysis. The width of the mid-rib of the middle leaflet of third trifoliate leaves of UVB excluded plants was found to be more compared to leaves of filter control plants, which are exposed to ambient UV. The mid-rib or the main conducting vein transports water and sugars to the whole plant; therefore, mid-rib enhancement by the exclusion of solar UV radiation possibly implies enhancement in the leaf area which in turn causes an increased rate of photosynthesis.

1. Introduction

The ultraviolet (UV) region of the electromagnetic radiation coming from sun is subdivided into three bands termed ultraviolet A (UVA; 315–400 nm), ultraviolet B (UVB; 280–315 nm) and ultraviolet C (UVC; 200–280 nm). UV radiation is of much interest to photo-biologists and has drawn their attention to studying the effects of UVB radiation on plants due to the depletion of the ozone layer. Most of the UVB and UVC radiation is absorbed by the stratospheric ozone layer, and therefore only UVA and a little UVB reaches the earth's surface (McKenzie *et al.*, 2011; Kataria *et al.*, 2014). Although UVB is a relatively minor component of sunlight, accounting for <0.5% of total light energy reaching the earth's surface, it has the highest energy of the daylight spectrum and therefore has a substantial impact on the biosphere. An elevation in the flux of UVB radiation is an environmental stress and has negative effects on plant growth and yield (Hollósy, 2002). In plants, leaves are the principle structures which are responsible for the manufacture of sugars, regulation of gas exchange, moisture and temperature. They are the main organs for performing evapotranspiration that moves water and nutrients up from the roots. They are also the organs that receive the major proportion of radiation under UVB



elevated environmental conditions and hence always react immediately to prevent its entry into internal organs (Bornman & Vogelmann, 1991; Rajendiran & Ramanujam, 2000).

The effects of the supplemental UVB on the cell structure have only been studied in a few growth chamber studies. The reported effects include decreased chloroplast, mitochondrial and starch volume density and increased thylakoid surface area in *Brassica napus* (Fagerberg & Bornman, 1997, 2005), and wrinkled thylakoid membranes, lumen dilations and damaged mitochondria in macroalgae (Holzinger *et al.*, 2004, 2006). Solar UVB radiation may induce morphological changes which include thicker leaves and shorter petioles, and affect anatomical development in leaves (Caldwell, 1981; Barnes *et al.*, 1990; Robson *et al.*, 2015).

More recent studies conducted on the exclusion of solar UV radiation have reported that such an exclusion significantly enhanced plant height and leaf area in many plant species (Amudha *et al.*, 2005; Kataria *et al.*, 2012a, 2013; Kataria & Guruprasad, 2014; Baroniya *et al.*, 2014) along with increased photosynthetic pigments and rate of photosynthesis (Laposi *et al.*, 2002; Amudha *et al.*, 2005; Guruprasad *et al.*, 2007; Kataria *et al.*, 2012b, 2013).

Brodribb *et al.* (2007) have reported the link between the rate of photosynthesis and the venation by leaf hydraulics. The imaging of the whole leaf structure (leaf venation architecture) facilitates understanding of the mechanism that interrelates leaf structure and hydraulic conductivity through intervessel connectivity. The transportation of water in the leaf tissues is due to the water potential gradient and water transport capacity known as the hydraulic conductance of leaves (Sack & Holbrook, 2006). The hydraulic architecture of leaves is a key determinant of water transport through the leaves (Cochard *et al.*, 2004). It is also reported that, irrespective of the leaf vascular anatomy, water flows through the low-resistance path in the vein network which is from the mid-rib to minor veins. Leaf parameters such as vein density have influence on the hydraulic efficiency and consequently on photosynthesis (Brodribb *et al.*, 2007). There are also reports on the effect of positioning of minor veins on the hydraulic efficiency (Brodribb *et al.*, 2007). So far, conventional imaging techniques have been used for vein pattern imaging. Over the past few decades intense research towards the contrast improvement in conventional X-ray imaging has resulted in the developments of phase contrast imaging techniques (Wilkins *et al.*, 1996; Zhou & Brahme, 2008; Arhatari *et al.*, 2005; Zoofan *et al.*, 2006).

In the phase contrast imaging technique the image contrast is obtained due to variation in the real part of the refractive index which is several orders of magnitude higher than the imaginary part responsible for absorption contrast. Hence, phase contrast imaging is most suitable for weakly absorbing samples (Davis *et al.*, 1995; Stevenson *et al.*, 2003; Wilkins *et al.*, 2014). The simplest implementation of the propagation-based phase contrast technique used here allows the incoming radiation to propagate in free space after interaction with the sample (Nesterets *et al.*, 2005; Weitkamp *et al.*, 2002; Mayo *et al.*,

et al., 2012). Synchrotron sources with a high degree of spatial and temporal coherence are more suitable for its implementation. High-intensity beam from a synchrotron source (synchrotron radiation) allows selection of wavelength which laboratory X-ray sources cannot provide. These unique properties of synchrotron radiation make it possible to obtain phase radiographs of thin samples including plants (Hwu *et al.*, 2002; Snigirev *et al.*, 1995). Synchrotron radiation has been used for studies of plant microstructure (Verboven *et al.*, 2015; Cloetens *et al.*, 2006; Lahlali *et al.*, 2015; Yamauchi *et al.*, 2013). High-quality images of the leaf vascular pattern using the synchrotron-radiation-based propagation phase contrast imaging technique are also reported (Blonder *et al.*, 2012). However, no information is available for studying the effect of solar UV exclusion on the structural changes of leaves.

Ambient UV radiation may induce structural and physiological changes in plants, influencing their growth and development. The present study involves the investigation of leaf vascular structure and main conducting vein (mid-rib) width variation upon solar UV exclusion using synchrotron-based X-ray phase contrast imaging. This technique is faster and non-destructive in visualization and measurement of the venation network. We hypothesized that ambient UV radiation would affect the width of the main conducting vein or mid-rib and the width of the connecting minor veins of the soybean leaves and affect the photosynthesis and thereby growth of leaves.

2. Methods

2.1. Plant material and experimental setup

The experiment was conducted under natural sunlight at the Terrace of School of Life Sciences, Devi Ahilya Vishwavidyalaya, Indore, India. Seeds of soybean (*Glycine max*) variety JS-335 were obtained from Directorate of Soybean Research, Indore (MP). The experiments were carried out from November 2014 to February 2015. The seeds were surface sterilized and then inoculated with slurry of *Rhizobium japonicum* strain before sowing in plastic nursery bags [34 cm height × 34 cm width; filled with a mixture of sand, black soil and manure (dried cow dung) in proportion 1:2:1]. Thereafter the nursery bags were immediately placed in iron mesh cages (1.2 m length × 0.91 m width × 0.91 m height). The cages were wrapped with UVB and UVAB cutoff filters (100 MIC Safety, Sun control film from Gareware Polyester Ltd., Mumbai, India) which specifically eliminate UVB (280–315 nm) and UVAB (280–400 nm) radiation, and the filter control plants were grown under an ordinary polythene filter that transmits all of the ambient solar radiation (filter control). The transmission of the filters measured using the Shimadzu spectrophotometer (UV-1601) is given in Fig. 1. The experiment was conducted in three replications each for control and treatments (exclusion of UVB and UVAB). The filters were erected from the time of germination and were maintained until maturity. The filters were replaced every two weeks as they became brittle because of solarization. The bottom sides

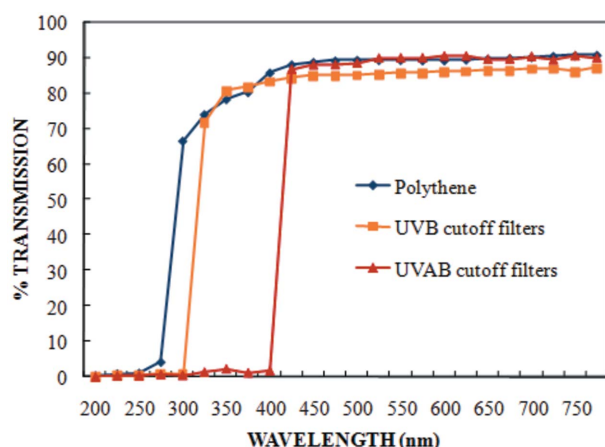


Figure 1
Transmission spectra of UV cutoff filters and polythene filter used for raising soybean plants variety JS-335 under iron mesh cages.

of all the cages (0.35 m above ground) were left uncovered to allow normal ventilation. The frames received full solar radiation for most of the day without any shading. Temperatures both inside and outside each enclosure were monitored daily using maximum/minimum thermometers. The average temperature outside rose from 25°C to 32°C during the growing period. No significant increase in temperature was measured inside the chambers compared with ambient air due to the passive ventilation system. Irrigation was provided as and when required for optimal growth of the crop.

2.2. Radiation measurement

Solar irradiance light was measured using a radiometer (IL 1350, International Light Inc., USA) between 1100 and 1200 hrs during the experimental period. The photosynthetic active radiation (PAR) during the experimental period at midday was 131 mW cm⁻² s⁻¹, the loss in light intensity at midday under polythene filter transmissible to UV (Filter Control) was 3.5% (126.5 mW cm⁻² s⁻¹), 22% (102 mW cm⁻² s⁻¹) by UVAB exclusion filters and 18% (107 mW cm⁻² s⁻¹) by UVB exclusion filters.

2.3. Leaf area and photosynthesis

Plants were sampled randomly in triplicate from all the treatments at 45 days after the emergence of seedlings (DAE).

The area of the middle leaflets of third trifoliate leaves of soybean was measured using the portable laser leaf area meter CID-202 scanning planimeter (CID Inc., USA). The rate of photosynthesis (P_N) was recorded using a portable infra-red gas analyser (LI-6200; LICOR Inc., Lincoln, USA) in the middle leaflets of third trifoliate leaves of plants grown in plastic bags between 1100 and 1200 hrs. Photosynthetic measurements were made in each treatment on clear days; the photosynthetic photon flux density (PPFD) was 1300–1600 $\mu\text{mol m}^{-2} \text{s}^{-1}$, with air flow 500 $\mu\text{mol s}^{-1}$ (Kataria & Guruprasad, 2014) and CO₂ concentration 350–380 p.p.m.

2.4. Phase contrast imaging technique

The imaging beamline BL-4 at the Indus-2 synchrotron radiation source was used to carry out imaging experiments (Agrawal *et al.*, 2015). A Si(111) type double-crystal monochromator was used to select suitable energy in the range 8–35 keV available from the broad white band of electromagnetic radiation. The synchrotron-based in-line phase contrast imaging set-up consists of motorized precision translation stages x , y and z and a rotation stage. The sample holder has a centrally fitted chuck for holding the samples. The imaging detector is a high-resolution CCD camera with an active area of 4000 by 2600 pixels; each pixel is 4.5 μm , with Gadox scintillator at its input face coupled to the CCD *via* fibre-optic 1:2 taper. Fig. 2 shows a schematic of the in-line phase contrast imaging set-up. The detector is also mounted on a long linear translation stage with 2 m translation to optimize the sample-to-detector distance for phase contrast optimization in in-line phase contrast imaging.

In the present study, images were obtained for third trifoliate leaves of soybean from each of the filter controls and treatments (exclusion of UVB and UVAB) (Fig. 3). The middle leaflets of third trifoliate leaves were mounted on a metallic frame horizontally to image the mid-rib region. Phase image contrast was optimized by varying the monochromatic beam energy in the range 8–20 keV and using a sample-to-detector distance (SDD) from 3 to 500 mm. Optimum phase contrast was obtained at an energy of 10 keV, a SDD of 300 mm and an exposure time of 1 s. Qualitative and quantitative analysis of the acquired images was carried out using *ImageJ* (<http://rsb.info.nih.gov/ij>) software. From the phase

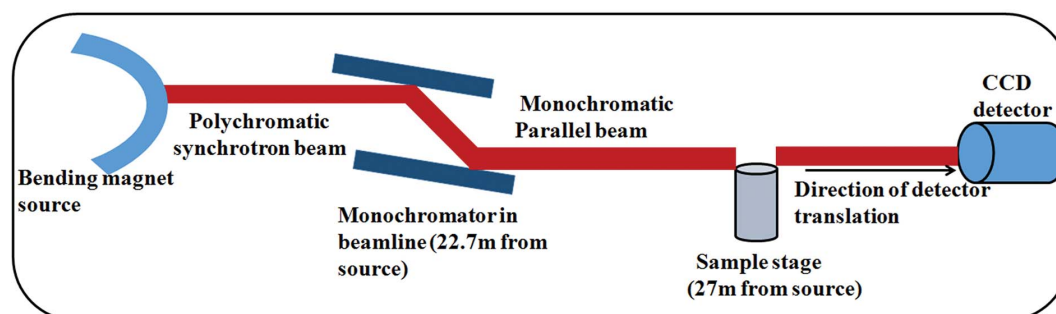


Figure 2
Schematic of the propagation-based phase contrast imaging set-up at the imaging beamline BL-4 at Indus-2.

Table 1

Exclusion of solar UVB and UVAB radiation induced effects on the area of the middle leaflet, width of the mid-rib, width of minor veins and area of the mid-rib along with minor veins of third trifoliolate leaves of soybean.

Data are the mean \pm standard error of the mean ($n = 3$). The numbers in parentheses are the percent changes with reference to respective filter controls.

Sample group	Area of middle leaflet (cm ²)	Average width of mid-rib (μ m)	Average width of minor veins (μ m)	Area of mid-rib + minor veins (mm ²)
Filter control	20 \pm 0.81	196.4 \pm 1.2	80.86 \pm 0.80	57.7 \pm 0.40
UVAB exclusion	34 [†] \pm 0.10 (+70)	279.1 [‡] \pm 2.0 (+42)	133.85 [†] \pm 0.90 (+65.5)	65.14 [†] \pm 1.2 (+12.8)
UVB exclusion	46 [†] \pm 0.12 (+130)	390.0 [†] \pm 2.2 (+98)	176.05 [†] \pm 1.01 (+117)	72.30 [†] \pm 1.1 (+25.3)

[†] Differences versus filter control significance at $P < 0.001$. [‡] Differences versus filter control significance at $P < 0.01$.

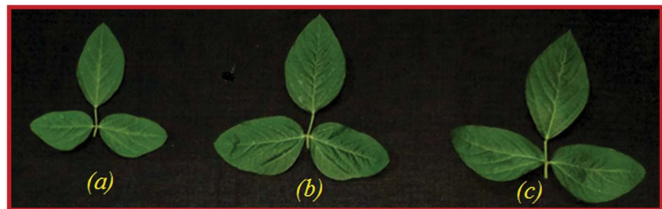


Figure 3 Soybean leaves (a) of the filter control, (b) under UVB excluded conditions and (c) under UVAB excluded conditions.

contrast images of each leaf, the mid-rib width was measured along the direction perpendicular to the length of the mid-rib at six places located at fixed intervals. An average mid-rib width was then obtained. A similar process was adopted for the quantification of minor veins visible in the images. All the phase contrast images of 7808 \times 1192 pixel size were segmented in *ImageJ* using the threshold process to separate the leaf skeleton containing mid-rib and minor veins. The resulting images obtained were used for finding the area of the mid-rib along with minor veins.

2.5. Statistical analysis

All the data are presented in triplicates ($n = 3$). The data are expressed as mean \pm standard error of the mean (SEM) and analyzed by the analysis of variance (ANOVA) followed by *post hoc* Newman–Keuls multiple comparison test ($*P < 0.05$, $**P < 0.01$, $***P < 0.001$) using *Prism 4* software for Windows (Graph Pad Software, LaJolla, CA, USA).

3. Results

3.1. Leaf area and photosynthesis

The exclusion of solar UVB and UVAB significantly ($P < 0.001$) enhanced the area of the middle leaflet of third trifoliolate leaves of soybean at 45 DAE as compared with the filter controls (Table 1). Exclusion of UVB promoted these parameters more efficiently than exclusion of UVAB (Table 1). The maximum enhancement of 70% and 130% in the area of the middle leaflet of third trifoliolate leaves was observed by the removal of UVAB and UVB, respectively (Table 1). Exclusion of solar UVB significantly ($P < 0.001$) enhanced the net rate of photosynthesis in the middle leaflet of third trifoliolate leaves of soybean (Fig. 4). The rate of photosynthesis (P_N) was

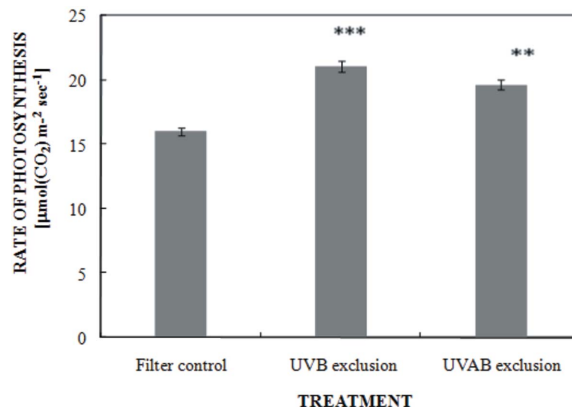


Figure 4 Rate of photosynthesis in soybean leaves under ambient, UVB excluded and UVAB excluded conditions. The vertical error bars indicate \pm standard error of the mean. Values are significantly different at ($**P < 0.01$, $***P < 0.001$) from the filter control (Newman–Keuls multiple comparison test).

enhanced by 31% after exclusion of solar UVB and 22% by solar UVAB exclusion (Fig. 4) as compared with the filter control.

3.2. Distance optimization in phase contrast imaging

The result of the synchrotron micro-imaging experiment shows images with high resolution and quality. The energy tunability at the synchrotron source allows contrast optimization at the desired level. An energy value of 10 keV was chosen for the leaf images so that an improved contrast at the mid-rib boundaries and vascular structure was seen. Fig. 5 shows mid-rib regions for the filter control using absorption and phase contrast imaging techniques. Absorption contrast images (Fig. 5a) were obtained by placing the sample as close as possible to the detector. The value of the contrast was calculated using the visibility formula (Born & Wolf, 1999) at the mid-rib boundaries. The maximum and minimum intensity values were taken from the intensity profile plots. At 3 mm SDD (Fig. 5a) the contrast was 7% and for 300 mm SDD (Fig. 5b) the contrast value obtained was 30.8%.

3.3. Comparison of mid-rib in phase contrast images

Fig. 6 shows the phase contrast images of the filter control; UVAB and UVB excluded conditions [Figs. 6(a)–6(c)]. Qualitative comparison of the mid-rib in Fig. 6 shows an

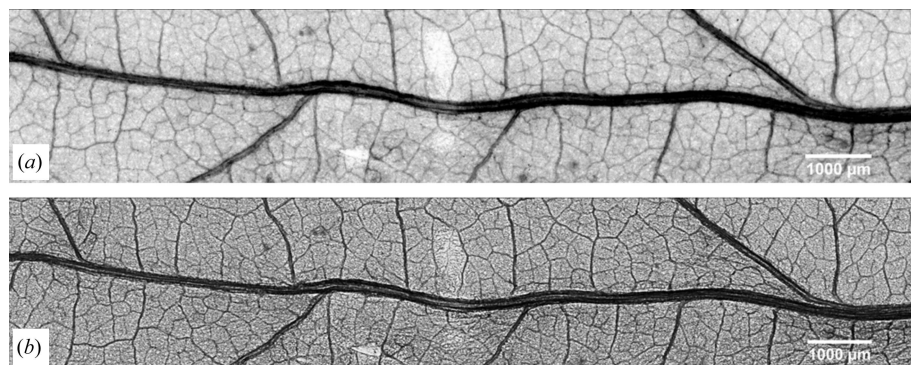


Figure 5
Mid-rib and vascular structure of the filter control soybean leaf. (a) Absorption image and (b) phase contrast image.

enhancement of mid-rib width in the middle leaflet of third trifoliate leaves grown under exclusion of UVAB and UVB [Figs. 6(b) and 6(c)]. Figs. 6(d)–6(f) show mid-rib enhancement with finer details in the inset. The phase contrast images also show minor vein structures with improved contrast.

Quantification of the mid-rib (major conducting vein) and minor vein from the phase contrast images indicates a larger mid-rib width for UVB excluded leaves (Table 1). The width of the mid-rib of the middle leaflet of third trifoliate leaves was increased by 98% and an increase of 117% was found in the width of minor veins of the middle leaflet of third trifoliate leaves after the exclusion of solar UVB (Table 1) as compared with the filter controls. The segmented phase contrast images for the filter control, exclusion of UVAB and UVB are shown

in Figs. 7(a)–7(c). The area of the mid-rib and minor veins measured after segmenting the phase contrast images also showed an increase by 25% after UVB exclusion (Table 1) as compared with the filter control.

4. Discussions

In the present study, the physical observation of leaves showed that exclusion of UVB and UVAB significantly enhanced their area and length, and the width and area of the mid-rib and minor veins of the middle leaflet of third trifoliate leaves of soybean at

45 DAE as compared with the filter controls. Enhancement of growth in terms of leaf area after the exclusion of the UVB component from the solar spectrum has been previously observed in several crop plants (Guruprasad *et al.*, 2007; Dehariya *et al.*, 2012; Kataria *et al.*, 2013; Zhang *et al.*, 2014).

Synchrotron imaging can be used to study leaf structure with a shorter data acquisition time and better resolution. This X-ray imaging has revealed primary and secondary veins with micrometre resolution sufficient to analyze the vascular structure. The leaf imaging performed in the present study requires no sample preparation like sectioning and staining. The technique allows imaging of intact leaf samples. The study of venation by this technique removes the difficulties of preparing and careful handling of the sections. The enhanced

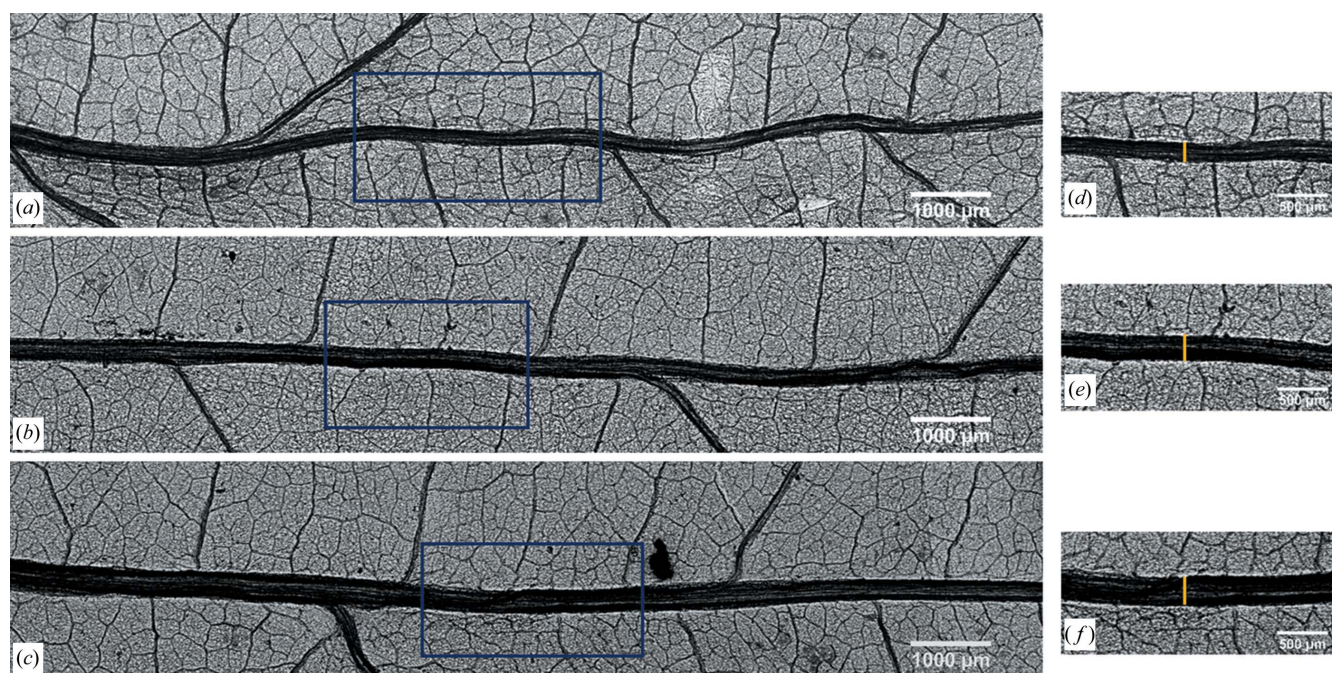


Figure 6
Phase contrast image of soybean leaf showing mid-rib and vascular structure. (a) Filter control (b) under UVAB excluded conditions and (c) under UVB excluded conditions; (d), (e) and (f) are enlarged views of the regions shown with blue rectangles in (a), (b) and (c), respectively; the width of the mid-rib is marked by the yellow line in these enlarged views.

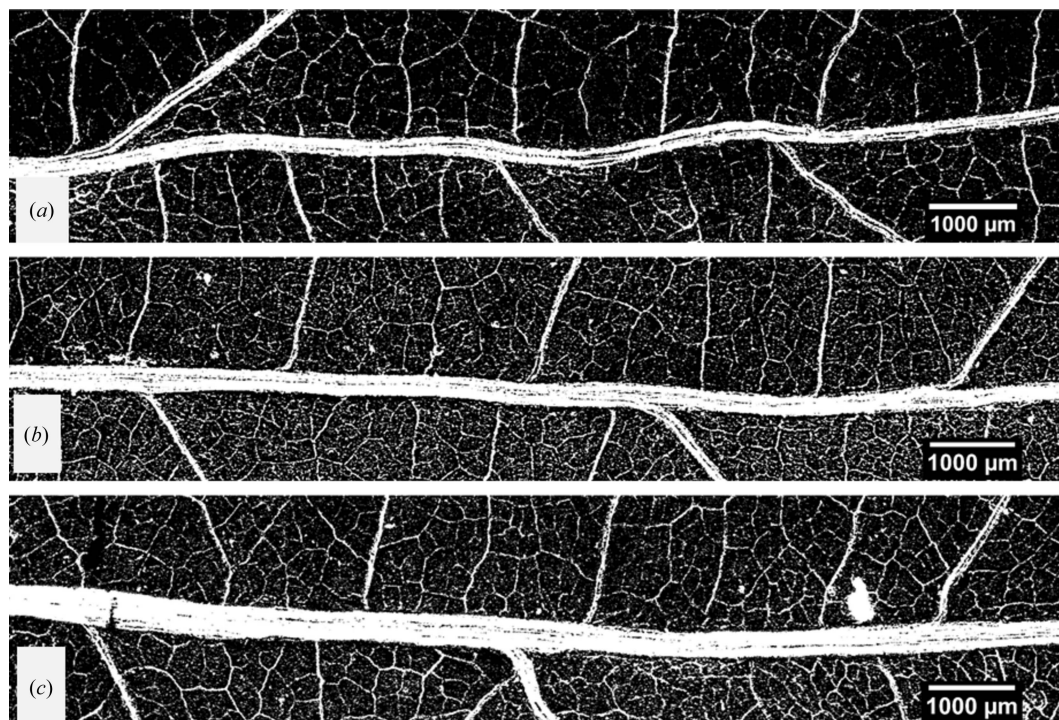


Figure 7
Phase contrast images after segmentation to separate leaf skeleton containing mid-rib and minor veins (a) of the filter control, (b) under UVAB excluded and (c) under UVB excluded conditions.

mid-rib width and area by the exclusion of solar UV components as confirmed from phase contrast imaging suggests an increased hydraulic efficiency that results in increased photosynthesis and enlarged leaf structures. These findings of synchrotron micro-imaging experiments agree with the photosynthesis results (Fig. 4).

The leaf hydraulic efficiency which is responsible for transport of water, nutrients and carbon in plants is enhanced during UV exclusion and the effects are displayed in the leaf venation architecture. These innovations resulted in large leaves with thicker major veins for mechanical support and a high vein length per unit area enabling transpirational cooling and high photosynthetic rates (Osborne *et al.*, 2004; Boyce, 2008; Brodribb *et al.*, 2010; Walls, 2011; Sack *et al.*, 2012). Leaf vein traits have numerous and increasing applications across a wide range of activities. Further integration of research on leaf venation across fields will hasten discoveries and generate a unified knowledge base across genetics, development, structure and function. This integration will contribute to a new understanding that extends across whole-plant biology and the ecology of current, past and future ecosystems. Leaf vascular system differentiation and venation patterns play a key role in transporting nutrients and maintaining the plant shape, which is an important agronomic trait for improving photosynthetic efficiency. However, there is little knowledge about the regulation of leaf vascular specification and development under UVB stress. Leaf vascular systems consist of a continuous network of interconnected cells throughout the leaf. Changes in internal leaf anatomy are related to changes in leaf

morphology. Species differ in their anatomical response to UVB radiation (Nagel *et al.*, 1998). Studying *Populus trichocarpa*, Schumaker *et al.* (1997) found that ambient UVB treatment resulted in thinner leaves compared with those of plants exposed to sub-ambient UVB radiation owing to decreased development of palisade parenchyma tissue. The improved visibility of vascular structure in the phase contrast images (Fig. 6) of UVB excluded leaves implies the thinning of leaves, and, also, the clear and wider mid-rib structure seen will allow increased hydraulic efficiency.

5. Conclusions

Increment in leaf venation structure caused by UV filtering has been imaged using the synchrotron hard X-ray phase contrast imaging technique with micrometre resolution. The study finds substantial increments in the leaf structure. There is an increment of 98% in width of the mid-rib of the leaves and 25% total area of vein structure. Parallel confirmation from photosynthetic studies has also been carried out. This study establishes hard X-ray phase contrast imaging as a potential nondestructive analysis tool for structural studies of botanical samples. This study in leaf venation has important implications for leaf physiological activity and hydraulic and light-utilization efficiency. Considering the substantial weight to leaf vein differentiation, the data presented here provide a basis for evaluating the structural changes associated with increasing the leaf photosynthetic rate, and the resultant impact on plant productivity after the solar UV exclusion.

Further work in this area will focus on other plants of interest to mankind.

Acknowledgements

Financial support by Board of Research in Nuclear Sciences project, BARC, Mumbai (No. 2009/34/52/BRNS) and UGC-MANF for subsequent fellowship to AF and Department of Science Technology Women Scientists A Scheme (SR/WOS-A/LS-674/2012-G) to SK are thankfully acknowledged.

References

- Agrawal, A. K., Singh, B., Kashyap, Y. S., Shukla, M., Sarkar, P. S. & Sinha, A. (2015). *J. Synchrotron Rad.* **22**, 1531–1539.
- Amudha, P., Jayakumar, M. & Kulandaivelu, G. (2005). *J. Plant Biol.* **48**, 284–291.
- Arhatari, B. D., Nugent, K. A., Peele, A. G. & Thornton, J. (2005). *Rev. Sci. Instrum.* **76**, 113704.
- Barnes, P. W., Flint, S. D. & Caldwell, M. M. (1990). *Am. J. Bot.* **77**, 1354–1360.
- Baroniya, S. S., Kataria, S., Pandey, G. P. & Guruprasad, K. N. (2014). *Crop J.* **2**, 388–397.
- Blonder, B., De Carlo, F., Moore, J., Rivers, M. & Enquist, B. J. (2012). *New Phytol.* **196**, 1274–1282.
- Born, M. & Wolf, E. (1999). *Principles of Optics*, 7th ed. Cambridge University Press.
- Bornman, J. F. & Vogelmann, T. C. (1991). *J. Exp. Bot.* **42**, 547–554.
- Boyce, C. K. (2008). *Paleontol. Soc. Papers*, **14**, 133–146.
- Brodribb, T. J., Feild, T. S. & Jordan, G. J. (2007). *Plant Physiol.* **144**, 1890–1898.
- Brodribb, T. J., Feild, T. S. & Sack, L. (2010). *Funct. Plant Biol.* **37**, 488–498.
- Caldwell, M. M. (1981). *Encyclopedia of Plant Physiology, Physiological Plant Ecology I: Responses to the Physical Environment I*, edited by O. L. Lange, C. B. Osmond and H. Zeigler, Vol. 12A, pp. 169–197. Berlin: Springer-Verlag.
- Cloetens, P., Mache, R., Schlenker, M. & Lerbs-Mache, S. (2006). *Proc. Natl Acad. Sci. USA*, **103**, 14626–14630.
- Cochard, H., Nardini, A. & Coll, L. (2004). *Plant Cell Environ.* **27**, 1257–1267.
- Davis, T. J., Gao, D., Gureyev, T. E., Stevenson, A. W. & Wilkins, S. W. (1995). *Nature (London)*, **373**, 595–598.
- Dehariaya, P., Kataria, S., Guruprasad, K. N. & Pandey, G. P. (2012). *Acta Physiol. Plant.* **34**, 1133–1144.
- Fagerberg, W. R. & Bornman, J. F. (1997). *Physiol. Plant.* **101**, 833–844.
- Fagerberg, W. R. & Bornman, J. F. (2005). *Photochem. Photobiol. Sci.* **4**, 275–279.
- Guruprasad, K., Kadur, G., Bhattacharjee, S., Swapan, B., Kataria, S., Sunita, K., Yadav, S., Sanjeev, Y., Tiwari, A., Arjun, T., Baroniya, S., Sanjay, B., Rajiv, A., Abhinav, R. & Mohanty, P. (2007). *Photosynth. Res.* **94**, 299–306.
- Hollós, F. (2002). *Micron*, **33**, 179–197.
- Holzinger, A., Karsten, U., Lütz, C. & Wiencke, C. (2006). *Phycologia*, **45**, 168–177.
- Holzinger, A., Lütz, C., Karsten, U. & Wiencke, C. (2004). *Plant Biol.* **6**, 568–577.
- Hwu, Y., Tsai, W., Groso, A., Margaritondo, G. & Je, J. H. (2002). *J. Phys. D*, **35**, R105–R120.
- Kataria, S. & Guruprasad, K. N. (2012a). *Field Crops Res.* **125**, 8–13.
- Kataria, S. & Guruprasad, K. N. (2012b). *Plant Sci.* **196**, 85–92.
- Kataria, S. & Guruprasad, K. N. (2014). *Sci. Hortic. (Amsterdam)*, **174**, 36–45.
- Kataria, S., Guruprasad, K. N., Ahuja, S. & Singh, B. (2013). *J. Photochem. Photobiol. B*, **127**, 140–152.
- Kataria, S., Jajoo, A. & Guruprasad, K. N. (2014). *J. Photochem. Photobiol. B*, **137**, 55–66.
- Lahlali, R., Karunakaran, C., Wang, L., Willick, I., Schmidt, M., Liu, X., Borondics, F., Forseille, L., Fobert, P. R., Tanino, K., Peng, G. & Hallin, E. (2015). *BMC Plant Biol.* **15**, 24.
- Laposi, R., Meszaros, I., Veres, S. & Mile, O. (2002). *Acta Biol. Szegediensis*, **46**, 243–245.
- McKenzie, R. L., Aucamp, P. J., Bais, A. F., Björn, L. O., Ilyas, M. & Madronich, S. (2011). *Photochem. Photobiol. Sci.* **10**, 182–198.
- Mayo, S. C., Stevenson, A. W. & Wilkins, S. W. (2012). *Materials*, **5**, 937–965.
- Nagel, L. M., Bassman, J. H., Edwards, G. E., Robberecht, R. & Franceschi, V. R. (1998). *Physiol. Plant.* **104**, 385–396.
- Nesterets, Y. I., Wilkins, S. W., Gureyev, T. E., Pogany, A. & Stevenson, A. W. (2005). *Rev. Sci. Instrum.* **76**, 093706.
- Osborne, C. P., Beerling, D. J., Lomax, B. H. & Chaloner, W. G. (2004). *Proc. Natl Acad. Sci. USA*, **101**, 10360–10362.
- Rajendiran, K. & Ramanujam, M. P. (2000). *National Symposium on Environmental Crisis and Security in the New Millennium*, edited by M. Khan, pp. 41–42. New Delhi: National Environmental Science Academy.
- Robson, T. M., Klem, K., Urban, O. & Jansen, M. A. K. (2015). *Plant Cell Environ.* **38**, 856–866.
- Sack, L. & Holbrook, N. M. (2006). *Annu. Rev. Plant Biol.* **57**, 361–381.
- Sack, L., Scoffoni, C., McKown, A. D., Frole, K., Rawls, M., Havran, J. C., Tran, H. & Tran, T. (2012). *Nat. Commun.* **3**, 837.
- Schumaker, M. A., Bassman, J. H., Robberecht, R. & Rademaker, G. K. (1997). *Tree Physiol.* **17**, 617–626.
- Snigirev, A., Snigireva, I., Kohn, V., Kuznetsov, S. & Schelokov, I. (1995). *Rev. Sci. Instrum.* **66**, 5486–5492.
- Stevenson, A. W., Gureyev, T. E., Paganin, D., Wilkins, S. W., Weitkamp, T., Snigirev, A., Rau, C., Snigireva, I., Youn, H. S., Dolbnya, I. P., Yun, W., Lai, B., Garrett, R. F., Cookson, D. J., Hyodo, K. & Ando, M. (2003). *Nucl. Instrum. Methods Phys. Res. B*, **199**, 427–435.
- Verboven, P., Herremans, E., Helfen, L., Ho, Q. T., Abera, M., Baumbach, T., Wevers, M. & Nicolai, B. M. (2015). *Plant J.* **81**, 169–182.
- Walls, R. L. (2011). *Am. J. Bot.* **98**, 244–253.
- Weitkamp, T., Rau, C., Snigirev, A. A., Benner, B., Gunzler, T., Kuhlmann, M. & Schroer, C. G. (2002). *Proc. SPIE*, **4503**, 92–102.
- Wilkins, S., Gureyev, T., Gao, D., Pogany, A. & Stevenson, A. (1996). *Nature (London)*, **384**, 335–338.
- Wilkins, S. W., Nesterets, Y. I., Gureyev, T. E., Mayo, S. C., Pogany, A. & Stevenson, A. W. (2014). *Philos. Trans. R. Soc. A*, **372**, 20130021.
- Yamauchi, D., Tamaoki, D., Hayami, M., Takeuchi, M., Karahara, I., Sato, M., Toyooka, K., Nishioka, H., Terada, Y., Uesugi, K., Takano, H., Kagoshima, Y. & Mineyuki, Y. (2013). *Microscopy*, **62**, 353–361.
- Zhang, L., Allen, L. H., Vaughan, M. M., Hauser, B. A. & Boote, K. J. (2014). *Agric. For. Meteorol.* **184**, 170–178.
- Zhou, S. & Brahme, A. (2008). *Phys. Med.* **24**, 129–148.
- Zoofan, B., Kim, J. Y., Rokhlin, S. I. & Frankel, G. S. (2006). *J. Appl. Phys.* **100**, 014502.